Ollscoil na Gaillimhe
University of Galway

Provided by the author(s) and University of Galway in accordance with publisher policies. Please cite the published version when available.

Title	Synthesis, characterization and reactivity of dyad ru-based molecules for light-driven oxidation catalysis
Author(s)	Farràs, Pau; Maji, Somnath; Benet-Buchholz, Jordi; Llobet, Antoni
Publication Date	2013-03-28
Publication Information	Farràs, P., Maji, S., Benet-Buchholz, J. and Llobet, A. (2013), Synthesis, Characterization, and Reactivity of Dyad Ruthenium-Based Molecules for Light-Driven Oxidation Catalysis. Chem. Eur. J., 19: 7162–7172. doi:10.1002/chem.201204381
Publisher	Wiley
Link to publisher's version	http:/dx.doi.org/10.1002/chem.201204381
Item record	http://hdl.handle.net/10379/5953
DOI	http://dx.doi.org/10.1002/chem.201204381

Downloaded 2024-04-23T18:47:00Z

Some rights reserved. For more information, please see the item record link above.

Synthesis, Characterization and Reactivity of Dyad Ru-Based Molecules for Light-Driven Oxidation Catalysis

Pau Farràs,[a] Somnath Maji,[a] Jordi Benet-Buchholz,[a] Antoni Llobet*[a,b]

Abstract: The synthesis of dyad molecules containing the 2,3,5,6-tetrakis(2-pyridyl)pyrazine (tppz) ligand of general formula $[(tpy)Ru(\mu\text{-}tppz)Ru(X)(L\text{-}L)]^{n+}$ where X = Cl, CF_3COO or H_2O and L-L = 2,2'-bipyridine (bpy) or 3,5-bis(2-pyridyl)pyrazole (Hbpp) and tpy is 2,2':6',2''-terpyridine have been prepared, purified and isolated. The complexes have been characterized by analytic and spectroscopic techniques and for two of them with X-ray diffractions analysis. Additionally, a full electrochemical characterization based on CV, DPV and SQWV has been also performed. The pH dependency of the redox couples for the aqua complexes have also been studied and their corresponding Pourbaix diagrams drawn. Furthermore their capacity to catalytically oxidize organic substrates such as alcohols, alkenes and sulfides has been carried out chemically, electrochemically and photochemically. Finally their capacity to behave as water oxidation catalysts has also been tested.

Keywords: ruthenium complexes • electron transfer • redox catalysis • water oxidation • water splitting • electrocatalysis • photocatalysis

Introduction

Solar fuels based on water splitting by sunlight is an attractive solution to today's energy problems.[1] Dyad molecules containing a light harvesting site and a water oxidation catalyst site combined are particularly attractive to incorporate in such systems. A few examples have been reported in the literature that can carry out redox transformation of organic substrates induced by light[2] but so far only two have been reported to be capable of oxidizing water to dioxygen in moderate yields.[3]

One of the potential strategies in this field is to build chromophore-catalyst "dyad" molecules with dinuclear Ru complexes represented as "Ru_PRu_C". One Ru center acts as light harvesting antenna, Ru_P, and the other center as water oxidation catalyst, Ru_C, and the two metals are connected by a bridging ligand. For these type of complexes, electron transfer from the light-harvesting antenna (Ru_P) to the active catalyst (Ru_C) can occur in an intramolecular manner through the bridging ligand. The latter will dictate the degree of electronic coupling between Ru_P and Ru_C and thus will be one of the crucial elements in this type of materials. Scheme 1 shows a few molecules, A-G, reported recently in the literature[2a-f,3a-b] of this type of complexes that have been shown to be capable of carrying out light induced oxidative transformations of external substrates.

In order to come out with efficient systems it is essential to understand in detail, at a molecular level, the large number of reactions that are involved in the light induced oxidative transformation. One of the key features of this type of molecules are the auxiliary ligands attached to the metal centers that will influence the energy of orbitals, the life time of the excited states, as well as

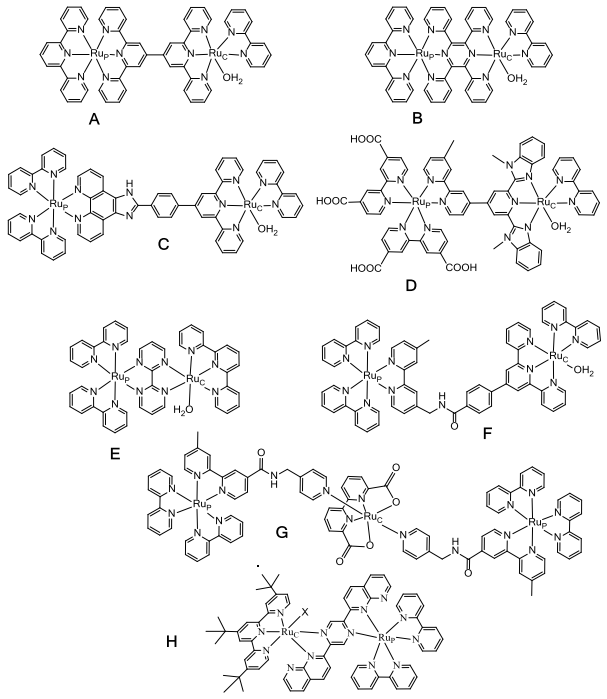

Scheme 1. Photocatalytically active Ru_PRu_C dyad molecules reported recently.

[a] Dr. P. Farràs, Dr. S. Maji, Dr. J. Benet-Buchholz, Prof. Dr. A. Llobet
Institute of Chemical Research of Catalonia (ICIQ)
Av. Països Catalans 16, E-43007 Tarragona, Spain
Fax: (+) 34 977920228
E-mail: allobet@iciq.es

[b] Prof. Dr. A. Llobet
Departament de Química
Universidad Autònoma de Barcelona
Cerdanyola del Vallès, 08193 Barcelona, Spain

the redox potentials of both sides. In addition the bridging ligand also plays a crucial role since besides the influences exerted by the auxiliary ligands just described, it can also produce an electronic coupling between the two metals. This degree of electronic coupling between the metal centers will cancel or favor desired reactions. With this degree of complexity it is imperative to have a sufficiently large pool of this type of complexes in order to understand the basic elements that govern their overall behavior. Theory can certainly help in the design of this type of molecules as was the objective of a recent work,[4] that gives some light to the effect of electronic coupling by a variety of bridging ligands.

The use photocatalytic methods for organic transformation is extraordinarily appealing both from a basic research point of view but also from a technological perspective. Oxidation of organic substrates, RH or RH_2, such as the ones described in equation 1 and 2,

$$RH_2 \xrightarrow{h\nu} R + H_2 \qquad (1)$$

$$H_2O + RH \xrightarrow{h\nu} R(O)H + H_2 \qquad (2)$$

are a very attractive concept for today's chemical industry. The successful scheme would avoid the need of environmentally harmful oxidants such as MnO_4^-, CrO_3, etc. that today are still used for organic oxidations,[5] and would generate H_2 as a very valuable byproduct.

The same type of scheme can be applied for the oxidation of water to dioxygen, as shown in equation 3.

$$2\,H_2O \xrightarrow{h\nu} O_2 + 2\,H_2 \qquad (3)$$

Altogether, photocatalytic oxidation of water and organic substrates is an area of great interest in both new energy conversion schemes and green chemistry since this could potentially reduce the use of hazardous chemicals and waste production, improve atom economy, and at the same time generate hydrogen as a very valuable fuel.[6]

With the aim to further gather crucial information in this subject we have prepared new dyad molecules containing the 2,3,5,6-tetrakis(2-pyridyl)pyrazine (tppz) ligand of general formula $[(tpy)Ru(\mu\text{-}tppz)Ru(X)(L\text{-}L)]^{n+}$ where X = Cl, CF_3COO or H_2O and L-L = 2,2'-bipyridine (bpy) or 3,5-bis(2-pyridyl)pyrazole (Hbpp) and tpy is 2,2':6',2"-terpyridine (see Scheme 2 for labeling scheme), and have characterized them by a combination of analytical, spectroscopic and electrochemical techniques. Furthermore we have tested their capacity to carry out photoinduced oxidation of organic substrates such as alcohols, sulfides and alkenes and also water.

Results and Discussion

Synthesis and Solid State Structure: The synthetic strategy followed to prepare complexes **1**–**7** is outlined in Scheme 2. Reaction of $[RuCl_3(tpy)]$ with the bridging ligand 2,3,5,6-tetrakis(2-pyridyl)pyrazine (tppz) generates the mononuclear complex $[Ru(tpy)(tppz)]^{2+}$, $\mathbf{1}^{2+}$ or Ru_P. This mononuclear complex reacts further with $RuCl_3$ to generate the dinuclear $[(tpy)Ru(\mu\text{-}tppz)RuCl_3]^{2+}$, $\mathbf{2}^{2+}$ or $Ru_PRu_CCl_3$, that is the synthetic intermediate used to prepare the rest of the complexes described in the present work. Now, $\mathbf{2}^{2+}$ can react with bidentate ligands such as bpy or Hbpp forming the corresponding Ru_PRu_CCl complexes $[(tpy)Ru(\mu\text{-}tppz)RuCl(bpy)]^{3+}$, $\mathbf{3}^{3+}$, and *in*- and *out*-$[(tpy)Ru(\mu\text{-}tppz)RuCl(Hbpp)]^{3+}$, *in*-$\mathbf{5}^{3+}$ and *out*-$\mathbf{5}^{3+}$ in a 30/70 ratio. For the latter the presence of the two isomers is due to the non-symmetric nature of the Hbpp ligand. Preparative TLC allows to isolate pure *out*-$\mathbf{5}^{3+}$ although the yield is only 15 %. For this reason a mixture of *in*- and *out*-$\mathbf{5}^{3+}$ was used to prepare the trifluoroacetato complex $[(tpy)Ru(\mu\text{-}tppz)Ru(CF_3COO)(Hbpp)]^{3+}$, $\mathbf{6}^{3+}$, and the mixture of isomers was solved by HPLC. Pure *out*-$\mathbf{6}^{3+}$ was now isolated with a 60 % yield.

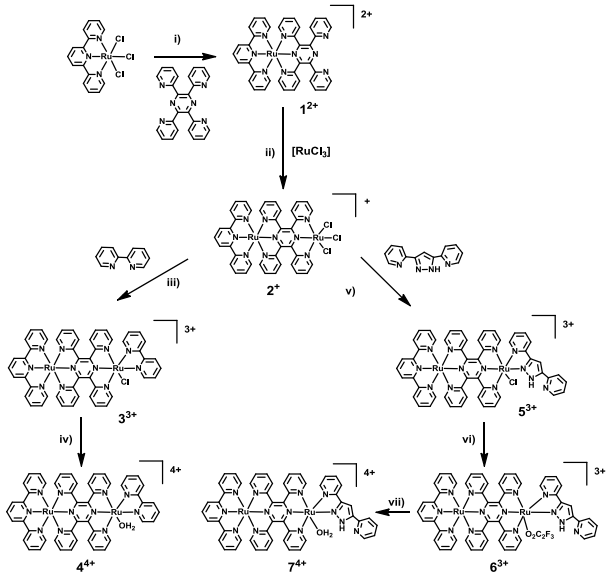

Scheme 2. i) NEt_3 in EtOH/water at reflux, isolation, then KPF_6 (excess) in water; 82% ($\mathbf{1}^{2+}$). ii) EtOH at reflux, isolation, then KPF_6 (excess) in water; 88% ($\mathbf{2}^{+}$). iii) 2,2'-bypiridine (1.0 equiv) in EtOH at reflux, then NH_4PF_6 (excess); 63% ($\mathbf{3}^{3+}$). iv) $AgClO_4$ (1.5 equiv) in acetone/water at reflux, then NH_4PF_6 (excess); 79% ($\mathbf{4}^{4+}$). v) 3,5-bis(2-pyridyl)-1H-pyrazole (Hbpp) (1.0 equiv) in EtOH at reflux, then NH_4PF_6 (excess); 20% (*out*-$\mathbf{5}^{3+}$). vi) prep. HPLC in CF_3COOH; 59% ($\mathbf{6}^{3+}$). vii) aqueous solution; 100% ($\mathbf{7}^{4+}$).

The preparation of Ru-aqua complexes, $Ru_PRu_COH_2$, $\mathbf{4}^{4+}$ and *out*-$\mathbf{7}^{4+}$ was achieved adding Ag^+ to $\mathbf{3}^{3+}$ for the former and by simply dissolving *out*-$\mathbf{6}^{3+}$ in neat water for the latter. The quantitative substitution of the trifloroacetato ligand by the aqua ligand occurs readily at room temperature as shown by ^{19}F NMR spectroscopy (see Sup. Inf.) The *out*-$\mathbf{7}^{4+}$ Ru-aqua complex was characterized in solution by UV-vis, NMR (^1H, ^{13}C, ^{19}F), MS and electrochemical techniques and was not isolated in the solid state. Complex $\mathbf{4}^{4+}$ has been recently reported by Rocha et al. using a different synthetic methodology with slightly lower yield.[2b]

Slow evaporation of an acetone:0.1 M triflic acid (1:4) solution of $\mathbf{4}^{4+}$ generates the monocrystals of the corresponding hydroxido complex, $[(tpy)Ru(\mu\text{-}tppz)Ru(OH)(bpy)]^{3+}$, Ru_PRu_COH. It is surprising to obtain the hydroxido complex in acidic media and this is most likely due to the much lower solubility of the hydroxido complex with regard to that of the aqua. Crystals of $\mathbf{5}^{3+}$ were obtained from a slow evaporation of a 1:1 solution of DCM:MeOH. Ortep views at 50% probability of the cationic moieties of complexes **4** and **5** are exhibited in Figure 1 together with their labeling scheme. Their crystallographic data are gathered in Table 1. Both crystal structures present a distorted octahedral geometry where the tppz ligand acts in a distorted meridional fashion, bpy or Hbpp ligands in a chelating fashion and finally the sixth

coordination position is occupied by the hydroxido or chlorido ligands. As already seen in other tppz bridged Ru complexes,[7] the tppz ligand adopts a saddle-shaped geometry with the pyrazine ring twisted across the metal–metal axis and with the pyridyl groups alternately displaced upward and downward around the pyrazine. The average dihedral angle formed between the intersection of the pyridyl planes with the pyrazine mean plane is 22.9º and 25.3º for Ru_PRu_COH and $\mathbf{5}^{3+}$, respectively. The bond distances and angles are unremarkable and thus similar to previous Ru complexes described in the literature.[8] Compound Ru_PRu_COH crystallizes in a two-dimensional porous structure that resembles that of a Metal Organic Framework (MOF) and is presented in Figure 2. It crystallizes in a large crystalline cell (trigonal space group R-3) which contains two dimensional channels that have a diameter of approximately 21 Å. These channels are filled with highly disordered water molecules. In this channel, for each MOF, 32 positions of water molecules (without hydrogen atoms) with different occupancies could be refined as shown in Figure 2. On the other hand, the most salient feature in $\mathbf{5}^{3+}$ is the hydrogen interaction between the chlorido ligand and the pyridylic CH from Hbpp (d_{CH} = 0.951 Å, d_{HCl} = 2.660 Å, d_{NCl} = 3.254 Å, $<_{CHCl}$ = 123.81º) depicted in Figure 1.

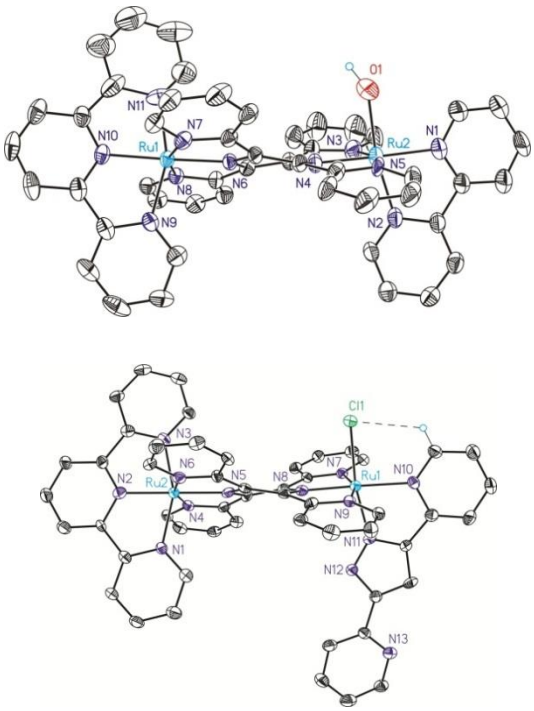

Figure 1. Ortep plot showing the molecular structure of the cationic part of complexes $[(tpy)Ru(\mu\text{-}tppz)Ru(OH)(bpy)]^{3+}$(up) (30% probability) and $\mathbf{5}^{3+}$(down) (50% probability). Non relevant Hydrogen atoms have been omitted for the sake of clarity. The interaction between Cl1 and H40 is shown for $\mathbf{5}^{3+}$.

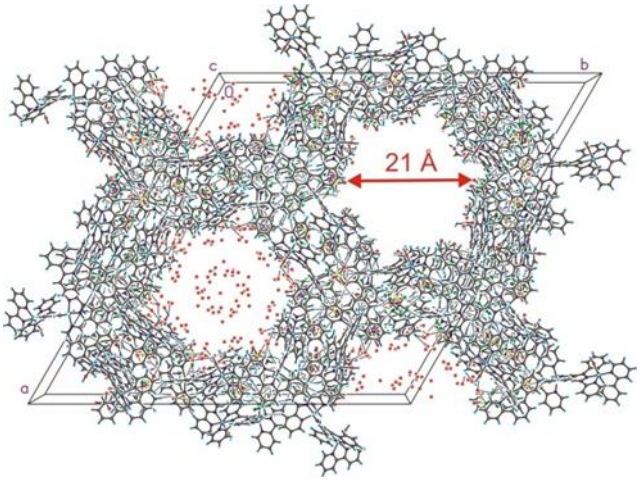

Figure 2. Drawing of the crystal packing of $[(tpy)Ru(\mu\text{-}tppz)Ru(OH)(bpy)](PF_6)_2(CF_3SO_3)\cdot 6H_2O$ showing the porous structure of the crystal. In the right channel the water molecules have been removed.

Spectroscopic Properties: 1D- and 2D-NMR spectroscopy on complexes $\mathbf{3}^{3+}$–$\mathbf{7}^{4+}$ in solution was carried out in order to fully characterize them, and the spectra are shown in the Sup. Inf. All resonances can be unambiguously assigned thanks to symmetry, integration, and their 2D spectra, and demonstrate that the molecular structure obtained in the solid state is maintained in solution, as expected for inert low-spin d_6-Ru^{II} type of cations. The most interesting feature of the spectra of the two Cl isomers is the strong downfield shift of H40 as a consequence of the strong Cl···H interaction ($d_{Cl\cdots H}$ = 2.66 Å), also seen in the crystal structure of $\mathbf{5}^{3+}$.

The electronic absorption spectroscopy and photochemical data for the complexes described in this work are listed in Table 2. The UV-vis spectra for $\mathbf{1}^{2+}$, $\mathbf{4}^{4+}$ and $\mathbf{7}^{4+}$ are presented in Figure 3. It is interesting to see how the dπ(Ru)- π*(tppz) MLCT band for $\mathbf{1}^{2+}$ is shifted to a single band at 550 nm for $\mathbf{4}^{4+}$ and $\mathbf{7}^{4+}$. This is due to the fact that the two main spectral components are averaged with absorption maxima at 550 nm, denoting significant charge delocalization across the tppz bridge and thus indicative of strong electronic coupling between the two metal centers.[2b]

Lifetimes emission for complexes $\mathbf{4}^{4+}$ and $\mathbf{7}^{4+}$ were found to be shorter than 2 ns in contrast to$[Ru(tpy)_2]^{2+}$ and related RuN_6 type of complexes that are in the range of microseconds. This lifetime decrease is attributed to the quenching of excited states by the Ru_C unit.

Table 1. Crystallographic Data for Complexes $\mathbf{4}(PF_6)_{2.25}(CF_3SO_3)_{0.75}$ and $\mathbf{5}(PF_6)(Cl)_2\cdot(CH_3COCH_3)_3\cdot(H_2O)_3$.

Empirical formula	$C_{49.75}H_{36}F_{15.75}N_{11}O_{3.25}P_{2.25}Ru_2S_{0.75}$	$C_{61}H_{61}Cl_3F_6N_{13}O_6PRu_2$
Formula weight	1435.00	1525.69
Temperature	100(2) K	100(2) K
Crystal system	Trigonal	Triclinic
Space group	*R*-3	*P*-1

Unit cell dimensions	a = 57.998(3) Å	a = 11.2523(9) Å
	b = 57.998(3) Å	b = 16.4813(11) Å
	c = 12.2786(8) Å	c = 18.7460(14) Å
	α= 90.00 °	α = 67.170(4) °
	β = 90.00 °	β = 87.165(5) °
	γ = 120.00 °	γ = 82.559(5) °
Volume	35769(4) $Å^3$	3177.2(4) $Å^3$
Z	18	2
Density (calculated)	1.199 Mg/m^3	1.595 Mg/m^3
Final R indices [I>2sigma(I)]	R1 = 0.0632 , wR2 = 0.1898	R1 = 0.0754 , wR2 = 0.1864
R indices (all data)	R1 = 0.0813 , wR2 = 0.1999	R1 = 0.1165 , wR2 = 0.2119

Redox Properties: Electrochemical experiments were carried out by means of Cyclic Voltammetry (CV), Differential Pulse Voltammetry (DPV) and Square Wave Voltammetry (SQWV) and are presented in Figures 4-6, 8, in Table 2 and in the Sup. Inf. For chlorido complexes $\mathbf{3}^{3+}$ and $\mathbf{5}^{3+}$ the voltammograms in DCM show two chemically reversible and electrochemically quasi-reversible redox waves assigned in the following equations,

$Ru_P^{II}Ru_C^{III}Cl + 1e^- \rightarrow Ru_P^{II}Ru_C^{II}Cl$ E^o = 1.03 V for $\mathbf{3}^{3+}$; 0.83 V for $\mathbf{5}^{3+}$ (4)

$Ru_P^{III}Ru_C^{III}Cl + 1e^- \rightarrow Ru_P^{II}Ru_C^{III}Cl$ E^o = 1.63 V for $\mathbf{3}^{3+}$; 1.56 V for $\mathbf{5}^{3+}$ (5)

The redox processes at 1.63 and 1.56 V for $\mathbf{3}^{3+}$ and $\mathbf{5}^{3+}$ are assigned to the $Ru^{III/II}$ couple of the photoactive unit Ru_P, given the similarity with that of $\mathbf{1}^{2+}$ (E^o = 1.43 V) and related $[Ru(tpy)_2]^{2+}$ type of complexes.[7b,7r] On the other hand, the redox couples at 1.03 and 0.83 V are assigned to the $Ru^{III/II}$ couple of the catalytic unit, given their similarity with Ru-Cl polypyridylic type of complexes such as $[Ru^{II}(Cl)(tpy)(bpy)]^+$, ($E^o$ = 0.92 V).[9] In the latter case the potentials are lower by approximately 200 mV given the less electron withdrawing character of bpy with regard to tppz. Finally the stronger σ-donating character of the Hbpp ligand produces a cathodic shift of roughly 200 mV for the $Ru^{III/II}$ couple of the Ru_C unit and a 70 mV cathodic shift to the more remote Ru_P unit. The latter manifests the existence of significant electronic coupling via the tppz bridging ligand that allows transmitting electron density by a distant F electron withdrawing group.

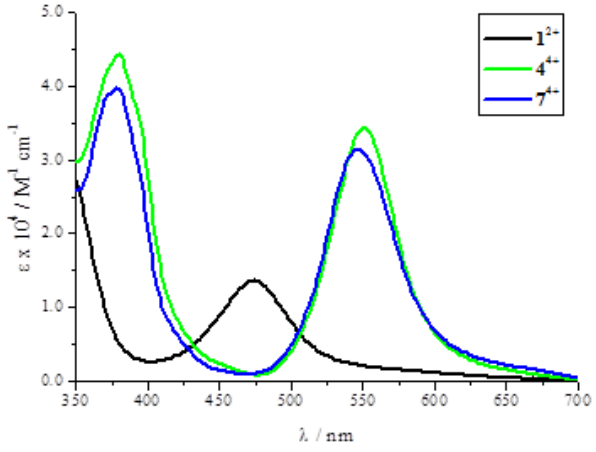

Figure 3. UV-vis spectra of 20 μM samples of complexes $\mathbf{1}^{2+}$ (black), $\mathbf{4}^{4+}$ (green) and $\mathbf{7}^{4+}$ (blue) at pH = 1.0 in a 0.1 M triflic acid solution.

The electrochemistry of complexes $\mathbf{4}^{4+}$ and $\mathbf{7}^{4+}$ have been investigated by CV and SQWV in the pH range 0.0-12.0. At pH = 1.0 in triflic acid $\mathbf{4}^{4+}$ presents four redox couples (see Figure 4) that are assigned as follows,

$Ru_P^{II}Ru_C^{III}OH_2 + 1e^- \rightarrow Ru_P^{II}Ru_C^{II}OH_2$ E^o = 0.96 V (6)

$Ru_P^{II}Ru_C^{IV}=O + 1e^- + 2H^+ \rightarrow Ru_P^{II}Ru_C^{III}OH_2$ E^o = 1.10 V (7)

$Ru_P^{III}Ru_C^{IV}=O + 1e^- \rightarrow Ru_P^{II}Ru_C^{IV}=O$ E^o = 1.19 V (8)

$Ru_P^{III}Ru_C^{V}=O + 1e^- \rightarrow Ru_P^{III}Ru_C^{IV}=O$ E^o = 1.35 V (9)

The last one is associated with an electrocatalytic current due to the oxidation of water to molecular dioxygen. In the case of $\mathbf{7}^{4+}$, the redox potentials appear at relatively similar potentials (see Sup. Inf.). The plot of E^o vs. pH or Pourbaix diagram is presented in Figure 5 and further gives support to the assignment in equations 6-9.

In a previous report the redox processes corresponding to equations 6-7 had been assigned[2b] but the processes at higher anodic potentials were not investigated. Furthermore, it was proposed that the first two waves due to the catalyst site, $Ru_P^{II}Ru_C^{III}OH/Ru_P^{II}Ru_C^{II}OH_2$ and $Ru_P^{II}Ru_C^{IV}O/Ru_P^{II}Ru_C^{III}OH$, were overlapped and appeared together at about 0.65 V vs. SCE at pH = 6.8. We have shown by SQWV that actually these are two separated 1 electron waves differing in only 140 mV in the pH range 1.8-8.2 (see Figure 4). Additionally comparison of the CV waves for a solution of ferricyanide with exactly the same concentration of $\mathbf{4}^{4+}$, shows practically the same intensity for the Fe(III/II) wave as the first wave ($Ru_P^{II}Ru_C^{III}OH_2/Ru_P^{II}Ru_C^{II}OH_2$) of $\mathbf{4}^{4+}$ at pH =1.0 (see Sup. Inf.). The lower intensity of the second wave ($Ru_P^{II}Ru_C^{IV}O/Ru_P^{II}Ru_C^{III}OH_2$) is associated with slow ET kinetics and is a feature that has also been reported in related Ru-aqua complexes.[10] To further analyze this subject we carried out open circuit potential (OCE) experiments that are reported in Figure 6. For $\mathbf{4}^{4+}$ the OCE = 0.65 V, upon addition of one equivalent of Ce(IV) the OCE increases to 0.95 V generating $[Ru^{II}{}_PRu_C^{III}OH_2]^{5+}$. A second addition of Ce(IV) generates $[Ru^{II}{}_PRu_C^{IV}O]^{4+}$ and the OCE jumps up to 1.07 V.

The tppz ligand is a strong π-acceptor ligand[7] and thus produces substantial anodic shifts at the Ru redox potentials. As a

Table 2. Thermodynamic, electronic absorption spectroscopy and photophysical data for complexes **1-7.**

Compd.	E^o [V]	λ_{max} [nm] (ε) [M^{-1} cm^{-1}]		assignment	λ_{max}^{em} [nm]	τ_{N2} [ns]
$\mathbf{1}^{2+}$	1.24,[a] 1.43[e]	271 (39700)	282 (38400)	π→π*	670[e]	28
		306 (48400)		dπ→π*	685[f]	21
		329 (44200)	350 (26000)	π→π*	650	-[g]
		474 (13800)		dπ→π*		
		560 (1900)		d→d		
$\mathbf{3}^{3+}$	1.03,[b] 1.63[a,e]	332 (45500)	370 (47470)	π→π*		
		440 (15120)	464 (13990)			
		582 (37890)		dπ→π*		
$\mathbf{4}^{4+}$	0.96,[b] 1.10,[c]	272 (51100)	284 (74800)	π→π*	600[f]	-[g]

	1.19,[a] 1.35[d]	298 (67500)	330 (29800)			
		348 (26200)				
		394 (28700)	546 (31500)	dπ→π*		
		678 (4500)		d→d		
5^{3+}	0.83,[b] 1.56[a,e]	-				
6^{3+}	0.92,[b] 1.46[e,h]	336 (34640)	375 (34420)	π→π*		
		396 (24030)	462 (5910)	dπ→π*		
		558 (26460)				
7^{4+}	0.84,[b] 1.09,[c]	272 (59600)	282 (66500)	π→π*	600[f]	-[g]
	1.19[a], 1.36[d]	298 (62500)	332 (33300)			
		366 (38200)	380 (43700)			
		396 (33700)	550 (34700)	dπ→π*		
		668 (4700)		d→d		

Redox couples measured at pH =1.0 (0.1 M aqueouis trifilic acid) corresponding to: [a] $Ru_P^{III/II}Ru_C^{IV}$, [b] $Ru_P^{II}Ru_C^{III/II}$, [c] $Ru_P^{II}Ru_C^{IV/III}$ and [d] $Ru_P^{III}Ru_C^{V/IV}$. [e] Measured in deoxygenated acetonitrile solution at room temperature. [f] Measured in a deoxygenated phosphate buffer (pH 7.0) solution at room temperature. [g] Lifetime shorter than laser response (< 2 ns). [h] Measured in acetone at room temperature.

consequence of this the Ru_C(III/II) ($Ru_P^{II}Ru_C^{III}OH_2/Ru_P^{II}Ru_C^{II}OH_2$) redox potential for the catalyst unit is above the thermodynamic value for the 4 electron water to oxygen potential by about 50 mV at pH = 7.0 (E^o = 0.73 V at pH = 7.0). Whereas typical Ru(III)-OH complexes such as $[Ru^{III}(tpy)(bpy)(OH)]^{2+}$, ($E^o_{III/II}$ = 0.48 V at pH = 7.0) are very stable and present limited reactivity with organic substrates, **4**$^{3+}$ reacts very fast with benzyl alcohol (BzOH) as can be observed in Figure 6 where the reactivity of $[Ru^{II}_PRu_C^{III}OH_2]^{5+}$ with BzOH is monitored by the OCE.

The stability of the Ru(III) oxidation state in 0.1 M triflic acid in the absence of any organic substrate was monitored by UV-vis spectroscopy. As can be observed in Figure 7 after 2 h, the complex returns back completely to its initial oxidation state Ru(II) with isosbestic points at 419, 459 and 534, following a first order kinetics with regard to Ru (k_{obs} = 4.01 x 10^{-4} s^{-1}). This experiment can be repeated several times without the apparent loss of Ru(II). This together with the absence of any organic substrate to be oxidized, points out that the reducing agent in this case is water, that in turn is oxidized to molecular dioxygen. Given the low overpotential for Ru(III)/Ru/(II) couple (34 mV) with regard to the thermodynamic H_2O to O_2 potential, and the 142 mV difference in the Ru_C(IV/III) vs. Ru_C(III/II) redox potentials, a plausible pathway could involve Ru_C(III) disproportion into Ru_C(II) and Ru_C(IV),

$2\ Ru_P^{II}Ru_C^{III}OH_2 \rightarrow Ru_P^{II}Ru_C^{II}OH_2 + Ru_P^{II}Ru_C^{IV}{=}O + 2H^+$

ΔG = 3.23 kcal/mol (K_{disp} = 4.29 x 10^{-3}) (10)

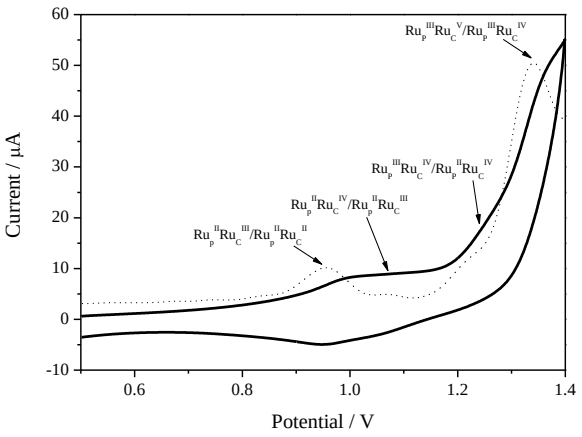

Figure 4. Redox properties of complex **4**$^{4+}$ in 0.1 M triflic acid using a glassy carbon disk electrode, Pt wire as auxiliary, and SSCE as reference electrode. The solid line is the CV performed at 10 mVs^{-1}. The dotted line is a SQWV of **4**$^{4+}$ (step E = 5 mV, SW amplitude = 20 mV, SW frequency=15 Hz).

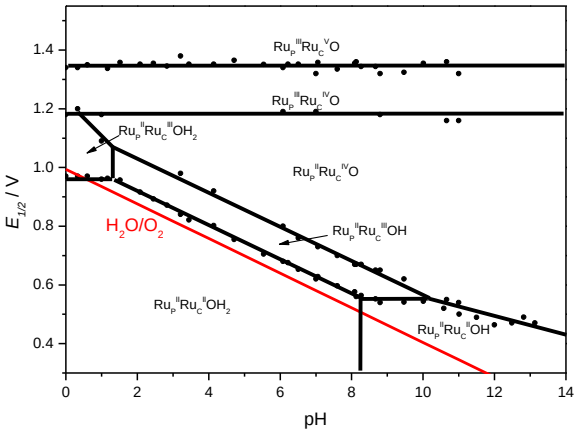

Figure 5. Pourbaix diagram for the aqua complex **4**$^{4+}$. The zones of stability of the different species as a function of the pH and $E_{1/2}$ (vs. SSCE) are shown and are indicated by the oxidation state of the ruthenium metal and the degree of protonation of the initial aqua group. The red line corresponds to the thermodynamic oxidation of water.

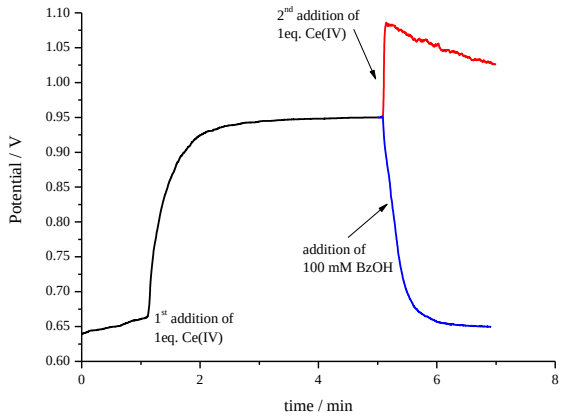

Figure 6. Open circuit potential graph versus time for complex **4**$^{4+}$ in a 0.1 M triflic acid solution at pH = 1.0. The black line shows the initial potential as well as the change upon addition of one equivalent of Ce(IV) to generate $[Ru^{II}_PRu_C^{III}OH_2]^{5+}$ species. The red line shows the effect of the addition of one equivalent of Ce(IV) to $[Ru^{II}_PRu_C^{III}OH_2]^{5+}$, generating $[Ru^{II}_PRu_C^{IV}O]^{4+}$ species. Finally the blue line shows the effect of adding benzyl alcohol (100 mM) to the $[Ru^{II}_PRu_C^{III}OH_2]^{5+}$ species in a separate experiment.

The first order behavior could imply that the rds is the O-O bond formation via water nucleofilic attack to $Ru_P^{II}Ru_C^{IV}O$ (we and others have previously obtained evidence for such a disproportion type of pathway[8c,11]). Once the $Ru_P^{II}Ru_C^{IV}O$ species is formed and water nucleophilic attack takes place, then a sequence of reactions can occur that finally can lead to the release of O_2. Other potential pathways involving an I2M mechanism could also be invoked.

The redox couple for $Ru_P^{II}Ru_C^{IV}O/Ru_P^{II}Ru_C^{III}OH_2$ is roughly 100 mV higher than for related potential for the benchmark complex $[Ru^{II}(tpy)(bpy)(OH_2)]^{2+}$ at pH = 1.0.[11] Given the fact that $Ru_C^{III}OH_2$ moiety is highly reactivity species one would expect that the further one electron oxidation would lead to even more reactive species. This is exactly what can be observe for the $Ru_P^{II}Ru_C^{IV}O$ in Figure 6, where in less than one minute a significant drop of the OCE is observed in the absence of any organic substrate. Furthermore the addition of BzOH generates an immediate decay of the OCE and thus manifests that $\mathbf{4}^{4+}$ is a powerful electrocatalyst. The CV experiments displayed in Figure 8 also show the electrocatalytic nature of $\mathbf{4}^{4+}$ in the presence of BzOH. A second order rate constant of $k_{cat} = 47.5\ M^{-1}s^{-1}$ has been calculated from the voltammograms in line with related active catalyst for this reaction (see Sup. Inf).[12]

As shown in the CV and SQWV $Ru_P^{III}Ru_C^{V}O$ is responsible for the electrocatalytic oxidation of water to dioxygen as it has also been proposed for $[Ru(tpy)(bpy)(H_2O)]^{2+}$ and related mononuclear complexes.[11] However and in sharp contrast with the previously discussed lower oxidation states, the redox potential at which this is occurring, 1.35 V *vs.* SSCE, is substantially lower than for most mononuclear complexes that occur in the range 1.46-1.57 V.[11] Therefore the combination of π-acceptor ligand such as tppz and the electronic coupling to the Ru_P moiety, modulated by the bridging tppz ligand, are responsible for lowering the redox potential which a priori seems counterintuitive.

It is important to realize here that the Ru(III/II) redox potential for the Ru_P unit is below that of the Ru(V/IV) redox potential of the Ru_C unit, and therefore for this dyad efficient photooxidation of water is discarded.

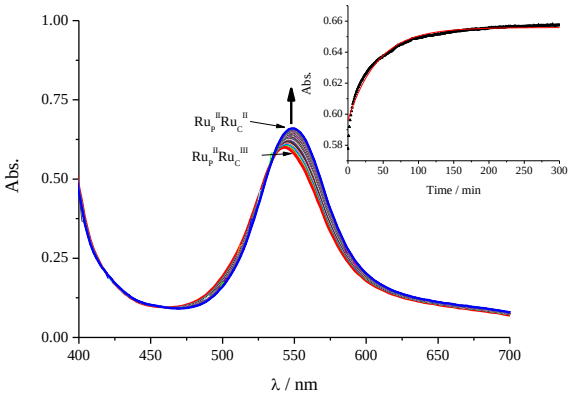

Figure 7. UV-vis spectral changes obtained for the decay $[(tpy)Ru^{II}(\mu\text{-}tppz)Ru^{III}(bpy)(OH_2)]^{5+}$, obtained upon addition of 1 equivalent of Ce(IV) to 2 mL of 0.02 mM $\mathbf{4}^{4+}$ at pH = 1.0 (data recorded every 60 s). The arrow indicates the absorption change at 550 nm. Inset: absorption *vs.* time plot at λ = 550 nm (diamonds) and mathematical simulation (red line) assuming a first order rate constant (k_{obs} = 4.01 x 10^{-4} s^{-1}). Isosbestic points at 419, 458 and 534 nm.

Catalytic Properties: Catalytic properties were investigated using chemical oxidants for the water oxidation reaction and for the oxidation of BzOH and methyl *p*-tolyl sulfide (MeSTol). Additionally photochemically induced oxidations were also carried out.

The aqua complexes $\mathbf{4}^{4+}$ and $\mathbf{7}^{4+}$ have been tested with regard to their capacity to catalytically oxidize water to molecular oxygen upon addition of a strong oxidant such as Ce(IV). Gas evolution has been monitored by both manometry, Clark electrodes in the liquid phase, and MS spectroscopy in the gas phase, and the results are shown in the Sup. Inf. The system $\mathbf{4}^{4+}$ 1 mM/Ce(IV) 100 mM/0.1M triflic acid with a total volume of 2 mL at 25.0 ºC gives 1.26 μmols of CO_2 and 1.14 μmols of O_2 (0.60 TN) after 20 min. On line MS shows that CO_2 and O_2 are generated simultaneously at the same rate and suggest that as the highly reactive $Ru_P^{III}Ru_C^{V}O$ active species are generated, the complex quickly degrades generating CO_2. It is interesting to note here that under identical condition the addition of Ce(IV) to $\mathbf{1}^{3+}$, does not generate any gases at all and thus indicates that Ce(IV) is not capable of reacting with neither the unbound nor the bonded part of the tppz ligand.

Under identical conditions, the Hbpp-based $\mathbf{7}^{4+}$ gives 0.4 μmols of CO_2 and 3.6 μmols of O_2 (2.0 TN).

It is interesting to compare here the dramatically different behavior of the dyads towards water oxidation with regard to their tpy mononuclear homologues: $[Ru(tpy)(bpy)(H_2O)]^{2+}$ and $[Ru(tpy)(Hbpp)(H_2O)]^{2+}$. Whereas the dyads are poor water oxidations and degrade very fast forming CO_2, their mononuclear homologues are efficient water oxidation catalysts. From these results it can be inferred that the dyads $\mathbf{4}^{4+}$ and $\mathbf{7}^{4+}$ are excellent catalysts for the oxidation of organic substrates which prevent them to be good WOCs.

The photocatalytic activity of complexes $\mathbf{4}^{4+}$ has been examined for the oxidation of a variety of organic substrates and the results obtained are presented in Table 3, together with the activity of related dyad complexes reported in the literature. Typically we use ratio of 1:500:1000 of catalyst:substrate:electron acceptor and a Xe lamp source (150 W) with a cut-off filter at λ>400 nm for 24 h in a thermostated jacketed cell.

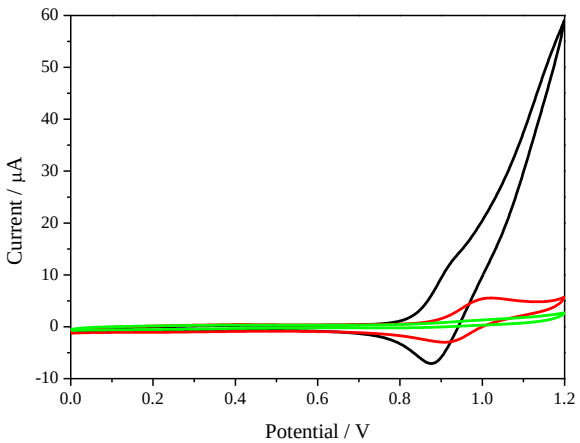

Figure 8. Cyclic voltammetry for $\mathbf{4}^{4+}$ (1.0 mM) at 0.01 V s^{-1} at pH = 1.0 in a deoxygenated 0.1 M triflic acid aqueous solution (red). After addition of 0.2 M benzyl alcohol (black). Blank with benzyl alcohol (green).

As can be observed in entries 1-4 of Table 3 for BzOH, the performance is strongly dependent on the temperature of the reaction. Actually the best performance in our case was obtained without the thermostated cell entry 5, that yields 38 TN with a conversion of 7.5%. This indicates that in this particular experiment the temperature of the experiment raised above 75°C. Under identical condition Rocha et al. for the same catalyst report a TN of 50 that can possibly be attributed to a temperature effect. It is worth mentioning here that using complex D (scheme 1), where the tppz bridging ligand is changed by the bis-tpy one, is capable of transforming 30% of the substrate giving a TN of 150. Finally the activity of complex $\mathbf{7}^{4+}$ (entry 7) under the same reaction conditions is very similar to that of $\mathbf{4}^{4+}$. Surprisingly using $[Ru(bpy)_3]^{2+}$ and $[Ru(trpy)(bpy)(H_2O)]^{2+}$ independently gave yields one order of magnitude higher (entry 9).

With regard to the oxidation of alkenes, one reaction test was carried out with *cis*-β-methylstyrene (entry 10, Table 3) with very low activities. A related complex F, was also tested giving even lower performance (entry 11, Table 3). The best performance for the photocatalytic transformation of alkenes has been achieved so far using a Mn-porphyrine catalyst in combination with $[Ru(bpy)_3]^{2+}$ as photosensitizer using a water soluble styrene as substrate.

Sulfides were also tested as substrates as indicated in entry 13, under the same conditions as the previous substrates giving a decent TN of 67 that represents a conversion of 13.4%. Related dyads give TN values of 124 and 201 TN for F and G respectively.

In conclusion, we have prepared new dyad molecules based on dinuclear Ru complexes, where one metal acts as light harvester, Ru_P, and the other one as oxidation catalysts, Ru_C. We have thoroughly characterized the new complexes spectroscopically and electrochemically. In addition we have shown that these complexes can act as photocatalysts for a variety of organic substrates such as alcohols, alkenes and sulfides. The fact that the $[Ru(bpy)_3]^{2+}$ and $[Ru(trpy)(bpy)(H_2O)]^{2+}$ independently work better than the dyads for the oxidation of BzOH, might be due to the fact that upon excitation the electron can be partially transferred to the bridging ligand, thus precluding the oxidation of the Ru_C site of the molecule. It thus puts forward the importance of the bridging ligand in dictating the photocatalytic performance of dyad type of molecules.

Table 3. Photocatalytic oxidation of a variety of substrates using $\mathbf{4}^{3+}$ and related dyad complexes in aqueous solution.[a]

Entry	Cat	Substrate	pH	t (h)	T (°C)	TN (Conv. %)	Ref[c]
1	-	BzOH	7.0	24	25	- (0.8)	Tw
2	-		7.0	8	75	- (1.2)	Tw
3	$\mathbf{4}^{4+}$		7.0	24	25	7 (1.4)	Tw
4	$\mathbf{4}^{4+}$		7.0	8	75	29 (5.8)	Tw
5	$\mathbf{4}^{4+}$		7.0	24	?[b]	38 (7.5)	Tw
6	$\mathbf{4}^{4+}$		7.0	24	?	50 (10.0)	2b
7	$\mathbf{7}^{4+}$		7.0	24	225	5.5 (1.1)	
8	D		7.0	24	?	150 (30.0)	2a
9	Sep[d]		7.0	6	25	50 (10.0)	
10	$\mathbf{4}^{4+}$	*cis*-PhCH=CHMe	7.0	24	25	11 (2.2)	Tw
11	E	*trans*-PhCH=CHMe	6.8	24	?	3 (0.6)	2e
12	-	PhSMe	7.0	24	25	- (5.5)	Tw
13	$\mathbf{4}^{4+}$		7.0	24	25	67 (13.4)	Tw
14	G		6.8	24	?	124 (24.8)	2e
15	F	4-Br-PhSMe	6.8	24	?	201 (40.2)	2c

[a] Reaction conditions: Catalyst 0.2 mM/Substrate 100 mM/$[Co^{III}(NH_3)_5Cl]^{2+}$ 200 mM irradiated with a Xenon lamp with a cutoff filter at 400 nm. [b] Same conditions as in entry 4 but with no thermostated cell. [c] Tw, means this work. [d] Mixing independently $[Ru(bpy)_3]^{2+}$ and $[Ru(trpy)(bpy)(H_2O)]^{2+}$.

Experimental Section

Materials: $RuCl_3 \cdot 3H_2O$ was supplied by Alfa Aesar and was used as received. Trifluoromethanesulfonic acid (99+%) was purchased from STREM/CYMIT. $[Ce^{IV}(NO_3)_6](NH_4)_2$ (Ce(IV)), tetra(2-pyridyl)pyrazine (tppz), 2,2'-bipyridine (bpy), 2,2':6',2''-terpyridine (tpy), KPF_6, triethylamine, NH_4PF_6, $AgClO_4$, $[Co(NH_3)_5Cl]Cl_2$, benzyl alcohol, phenyl methyl sulfide, *cis*-β-methylstyrene and all organic solvents were of the highest purity commercially available and were used as received from Aldrich or Acros/Fisher. Aqueous solutions were prepared by using deionized water from an Ultra Clear water purifier system from SG Wasseraufbereitung und Regenerierstation GmbH (Conductivity at 25 °C = 0.055 μScm^{-1}).

Preparations: $[RuCl_3(tpy)]$,[13] $\mathbf{1}[PF_6]_2$[14] and $\mathbf{2}[PF_6]$[15] were prepared by following literature procedures. All synthetic manipulations were routinely performed under a nitrogen atmosphere using Schlenk tubes and vacuum-line techniques. NMR assignment of synthesized compounds can be found in Figure 9.

Synthesis of complexes [(tpy)Ru(μ-tppz)Ru(bpy)(Cl)](PF$_6$)$_3$·CH$_2$Cl$_2$·3H$_2$O, 3$(PF_6)_3 \cdot CH_2Cl_2 \cdot 3H_2O$**.** A mixture of $[(tpy)Ru(\mu\text{-}tppz)RuCl_3](PF_6)$ (0.200 g, 0.186 mmol) and 2,2'-bipyridine (0.030 g, 0.192 mmol) in ethanol (50 mL)were refluxed for 8h. After cooling to room temperature the mixture was concentrated by rotary evaporation and added dropwise excess saturated aqueous solution of NH_4PF_6. The resulting precipitate was separated from the solution by vacuum filtration, washed with little portions of chilled water and diethyl ether (50 mL), and dried under vacuum. This crude product was then purified by neutral alumina column using an acetone/DCM (2/1) solvent mixture. The desired product eluted first as a dark blue band, which was then concentrated by rotary evaporation and vacuum dried. Yield: 186 mg (63%). ^{1}H NMR (400 MHz, acetone-d$_6$): δ = 10.36 (d, *J* = 6, H10), 9.26 (d, *J* = 8, H43), 9.26 (d, *J* = 8, H41), 9.23(d, *J* = 8, H31), 9.20 (d, *J* = 8, H26), 9.19 (d, *J* = 8, H14), 9.18 (d, *J* = 8, H21), 9.12 (d, *J* = 8, H7), 8.96 (d, *J* = 8, H38), 8.89 (d, *J* = 8, H46), 8.82 (d, *J* = 8, H4), 8.75 (t, *J* = 8, H42), 8.63 (t, *J* = 8, H8), 8.27 (t, *J* = 6, H37), 8.27 (d, *J* = 6, H11), 8.25 (t, *J* = 6, H9), 8.22 (d, *J* = 7, H24), 8.21 (t, *J* = 8, H23), 8.15 (d, *J* = 8, H35), 8.12 (t, *J* = 6, H27), 8.12 (t, *J* = 6, H32), 8.10 (t, *J* = 7, H47), 8.08 (d, *J* = 8, H49), 8.07 (t, *J* = 6, H13), 8.07 (t, *J* = 6, H22), 8.03 (t, *J* = 8, H3), 7.97 (t, *J* = 6, H1), 7.70 (t, *J* = 6, H48), 7.70 (t, *J* = 6, H36), 7.54 (t, *J* = 6, H28), 7.54 (d, *J* = 8, H29), 7.52 (d, *J* = 8, H34), 7.44 (t, *J* = 6, H33), 7.35 (t, *J* = 6, H12), 7.24 (t, *J* = 6, H2); ^{13}C{^{1}H} NMR (62.9 MHz, acetone-d$_6$): δ = 158.00 (C34), 157.78 (C29), 156.12 (C11), 155.64 (C10), 155.13 (C49), 154.17 (C35), 153.31 (C1), 152.67 (C24), 138.90 (C22), 138.61 (C8), 138.12 (C32), 137.83 (C42), 137.39 (C13), 137.16 (C3), 128.64 (C28), 128.19 (C33), 127.93 (C12), 127.47 (C23), 127.10 (C2), 124.92 (C38), 124.51 (C31), 124.36 (C14), 124.29 (C7), 123.87 (C4); ESI MS (+) in CH_3CN *m/z* calcd.: 1306.02; found: 1305.8 [*M*-PF$_6$]$^+$; elemental analysis calcd. (%) for $C_{49}H_{35}ClF_{18}N_{11}P_3Ru_2 \cdot CH_2Cl_2 \cdot 3H_2O$: C 37.79, H 2.73, N 9.69; found: C 38.09, H 2.73, N 9.48.

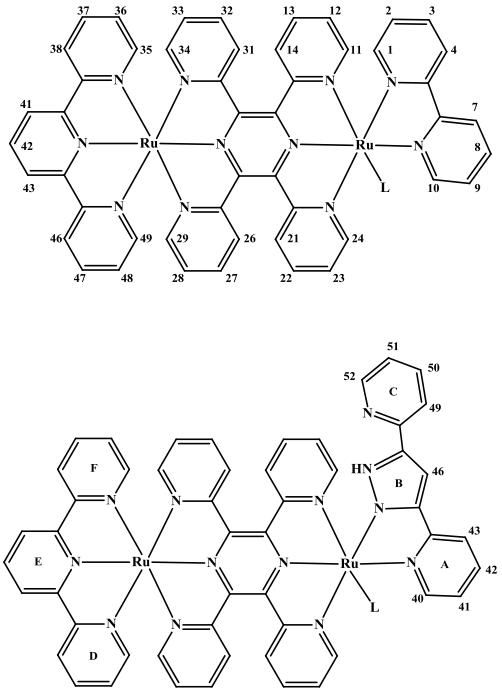

Figure 9. Numbering scheme for NMR assignment for complexes **3**-**7**.

[(tpy)Ru(μ-tppz)Ru(bpy)(H$_2$O)](PF$_6$)$_4$·6H$_2$O; 4(PF$_6$)$_4$·6H$_2$O**:** The chlorido complex **3**(PF$_6$)$_3$·CH$_2$Cl$_2$·3H$_2$O (0.100 g, 0.063 mmol) and AgClO$_4$ (0.022 g, 0.106 mmol) were heated together under reflux for 2 h in a mixture of acetone/water (3/1) (40 mL). AgCl was filtered off and the solution volume reduced to 5 mL on a rotary evaporator and added dropwise excess saturated aqueous NH_4PF_6. The resulting dark purple red precipitate was separated from the solution by vacuum filtration, washed with little portions of chilled water and diethyl ether (50 mL), and dried under vacuum. Yield: 84 mg (79%). ^{1}H NMR (400 MHz, D$_2$O): δ = 9.53 (d, *J* = 5, 1H), 8.94 (d, *J* = 8, 4H), 8.87 (d, *J* = 8, 1H), 8.83 (d, *J* = 8, 1H), 8.82 (d, *J* = 8, 1H), 8.60 (d, *J* = 8, 1H), 8.52 (t, *J* = 8, 2H), 8.46 (t, *J* = 8, 2H), 8.13 (t, *J* = 6, 1H), 8.06 (broad, 1H), 7.77-8.00 (m, 9H), 7.72 (d, *J* = 6, 2H), 7.60 (d, *J* = 6, 1H), 7.53 (broad, 2H), 7.44 (d, *J* = 6, 1H), 7.32 (t, *J* = 7, 2H), 7.23 (t, *J* = 7, 1H), 7.06 (t, *J* = 7, 2H); ^{13}C{^{1}H} NMR (62.9 MHz, acetone-d$_6$): δ = 158.46, 158.28, 157.71, 156.54, 155.54, 155.10, 154.84, 154.22, 154.11, 153.34, 152.55, 152.18, 150.64, 139.16, 138.30, 138.21, 137.78, 130.10, 129.28, 128.14, 128.05, 127.72, 127.29, 125.08, 124.52, 124.47, 124.11, 123.91;ESI MS (+) in H$_2$O *m/z* calcd.: 1416.01; found: 1415.7 [*M*-PF$_6$-H$_2$O]$^+$; elemental analysis calcd.(%) for C$_{49}$H$_{37}$F$_{24}$N$_{11}$OP$_4$Ru$_2$·6H$_2$O: C 34.91, H 2.93, N 9.14; found: C 34.96, H, 2.61, N 9.16.

***out*-[(tpy)Ru(μ-tppz)Ru(Hbpp)(Cl](PF$_6$)$_3$·2H$_2$O,** *out*-**5**(PF$_6$)$_3$·2H$_2$O. A mixture of [(tpy)Ru(μ-tppz)RuCl$_3$](PF$_6$) (0.200 g, 0.186 mmol) and Hbpp ligand (0.042 g, 0.189 mmol) in ethanol (50 mL) were refluxed for 12 h. After cooling to room temperature the mixture was concentrated by rotary evaporation and added dropwise excess saturated aqueous NH_4PF_6. The resulting precipitate was separated from the solution by vacuum filtration, washed with little portions of chilled water and diethyl ether (50 mL), and dried under vacuum. This crude product was then purified by neutral alumina column using an acetone/DCM (1/1) solvent mixture. The desired product was eluted first as a dark blue band, which was then concentrated by rotary evaporation and vacuum dried. The ^{1}H-NMR of the reaction mixture showed that a mixture of *in* and *out* isomers was obtained. The *out* isomer was isolated by chromatographic separation using preparative alumina TLC plate in a DCM/acetone mixture (4/1). Yield: 15 mg (10%).^{1}H NMR (400 MHz, methanol-d$_4$): δ = 10.07 (d, *J* = 6, 1H), 9.07 (t, *J* = 8, 2H), 9.00 (t, *J* = 9, 4H), 8.82 (d, *J* = 8, 1H), 8.79 (d, *J* = 8, 1H), 8.62 (t, *J*= 8, 1H), 8.44 (d, *J* = 6, 1H), 8.36 (t, *J* = 6, 2H), 8.32 (t, *J* = 8, 1H), 8.20 (broad, 2H), 8.10 (t, *J* = 8, 1H), 8.07 (t, *J* = 8, 1H), 7.98 (d, *J* = 8, 2H), 7.95 (d, *J* = 8, 2H), 7.90 (d, *J* = 6, 1H), 7.84 (t, *J* = 6, 1H), 7.77 (d, *J* = 6, 2H), 7.61 (t, *J* = 7, 2H), 7.56 (d, *J* = 8, 1H), 7.52 (d, *J* = 8, 1H), 7.43 (t, *J* = 6, 2H), 7.42 (s, 1H), 7.35 (t, *J* = 8, 1H), 7.30 (d, *J* = 6, 1H), 7.12 (t, *J* = 6, 1H); ESI MS (+) in MeOH *m/z* calcd.: 1371.03; found: 1371.7 [*M*-PF$_6$]$^+$; elemental analysis calcd. (%) for C$_{52}$H$_{37}$ClF$_{18}$N$_{13}$P$_3$Ru$_2$·2H$_2$O: C 40.23, H 2.66, N 11.73; found: C 40.13, H 2.73, N 11.58.

***out*-[(tpy)Ru(μ-tppz)Ru(Hbpp)(CF$_3$COO)](PF$_6$)$_3$·4H$_2$O,** *out*-**6**(PF$_6$)$_3$·4H$_2$O. The reaction mixture **5**(PF$_6$)$_3$·2H$_2$O (100mg, 0.064 mmol) was separated by reverse phase semi preparative TLC using H$_2$O (containing 0.1% CF$_3$COOH)/acetone (95/5) mixture as an eluent, leading to the *out*-**6**(PF$_6$)$_3$·4H$_2$O complex as the final product. Yield: 63 mg (59%). ^{1}H NMR (400 MHz, acetone-d$_6$): δ = 10.31 (d, *J* = 5.5, 1H Hbpp H40), 9.20 (d, *J* = 8, 1H tpy ring E), 9.16 (t, *J* = 6, 1H tppz), 9.14 (t, *J* = 6.6, 2H tppz), 9.03 (d, *J* = 7, 2H Hbpp ring A, C), 8.95 (d, *J* = 8, 1H tpy ring F), 8.89 (d, *J* = 8, 1H tpy ring D), 8.70 (t, *J* = 8, 1H tpy ring E), 8.44 (d, *J* = 5, 2H tppz), 8.32 (t, *J* = 8, 1H tppz), 8.26 (d, *J* = 8, 1H tppz), 8.23 (t, *J* = 3, 2H tppz), 8.19 (t, *J* = 8, 1H tpy ring F), 8.05 (t, *J* = 7, 3H tppz), 8.02 (d, *J* = 5, 2H tpy ring D + Hbpp), 7.99 (t, *J* = 7, 3H tpy ring D + Hbpp+ tppz), 7.89 (t, *J* = 6, 1H tppz), 7.70 (t, *J* = 6.6, 2H tppz), 7.50 (t, *J* = 6.6, 2H Hbpp), 7.42 (t, *J* = 6.6, 1H tpy ring F, 7.35 (s, 1H Hbpp H46), 7.02 (t, *J* = 6.2, 1H tpy ring D), 6.92 (d, *J* = 6, 1H tppz), 6.80 (t, *J* = 5, 2H tppz);^{13}C{^{1}H} NMR (62.9 MHz, acetone-d$_6$): δ = 158.15, 156.64, 155.66, 155.58, 154.90, 154.23, 153.99, 153.27, 152.96, 152.61, 150.76, 149.46, 148.91, 146.37, 138.67, 138.39, 138.02, 137.10, 135.59, 135.21, 128.28, 128.12, 127.85, 127.28, 124.79, 124.33, 124.19, 122.14, 120.57, 119.73, 118.44, 102.05; ESI MS (+) in H$_2$O *m/z* calcd.: 652.54; found: 652.4 [*M*-2PF$_6$/2]$^{2+}$; elemental analysis calcd.(%) for C$_{54}$H$_{37}$F$_{21}$N$_{13}$O$_2$P$_3$Ru$_2$·4H$_2$O: C 38.93, H 2.72, N 10.93;found: C 38.69, H 2.57, N, 10.58.

***out*-[(tpy)Ru(μ-tppz)Ru(Hbpp)(H$_2$O)](PF$_6$)$_4$, *out*-7**(PF$_6$)$_4$**:** This complex is prepared quantitatively upon dissolving *out*-**6**(PF$_6$)$_3$·4H$_2$O in an aqueous solution. ^{1}H NMR (400 MHz, D$_2$O): δ = 9.84 (d, *J* = 5.2, 1H), 8.87 (d, *J* = 8.4, 2H), 8.81 (d, *J* = 8, 2H), 8.79 (d, *J* = 8.4, 2H), 8.54 (d, *J* = 8.7, 1H), 8.48 (t, *J* = 8.7, 2H), 8.44 (d, *J* = 8, 2H), 8.31 (t, *J* = 7, 2H), 8.07 (broad, 2H), 7.94-7.29 (m, 8H), 7.65 (d, *J* = 5, 2H), 7.58 (s, 1H), 7.55 (t, *J* = 5, 2H), 7.46 (t, *J* = 4, 2H), 7.32 (t, *J* = 6, 1H), 7.24 (t, *J* = 6, 2H), 7.11 (t, *J* = 6.5, 1H), 7.05 (t, *J* = 7, 1H);^{13}C{^{1}H} NMR (62.9 MHz, acetone-d$_6$): δ = 158.32, 158.05, 157.68, 156.77, 156.08, 155.65, 155.33, 154.75, 154.37, 153.95, 153.36, 150.89, 149.17, 139.19, 139.11, 138.97, 138.29, 138.22, 138.12, 138.02, 129.53, 129.42, 129.23, 128.55, 128.25, 128.07, 125.13, 125.00, 124.80, 124.63, 124.43, 124.30.

Instrumentation and Measurements: UV-vis spectroscopy was performed on a Cary 50 (Varian) UV-Vis spectrophotometer in 1 cm quartz cuvettes. The NMR spectroscopy experiments were performed on a Bruker Avance 400 Ultrashield NMR spectrometer. Samples were run in d$_1$-chloroform, D$_2$O or d$_6$-acetone with internal references (residual protons). Elemental analysis was performed using an EA-1108, CHNS-O elemental analyzer from Fisons Instruments. ESI-MS analyses were recorded on an esquire 6000 ESI ion Trap LC/MS (Bruker Daltonics) equipped with an electrospray ion source. Cyclic voltammetry (CV), Differential Pulse Voltammetry (DPV) and Square-Wave Voltammetry (SQWV) experiments were performed in a IJ-Cambria IH-660C potentiostat using a three-electrode cell. A glassy carbon electrode (2 mm diameter) was used as working electrode, platinum (2 mm diameter) as auxiliary electrode, and SSCE as a reference electrode. Working electrodes were polished with 0.05 micron Alumina paste and washed with distilled water and acetone followed by blow-drying, before each measurement. All cyclic voltammograms presented in this work were recorded in the absence of light and inside a Faradaic cage. The complexes were dissolved either in CH_2Cl_2 (DCM) or CH_3CN (ACN) containing the necessary amount of nBu$_4$NPF$_6$ (TBAH) as supporting electrolyte to yield a 0.1 M ionic strength solution. In aqueous solution the electrochemical experiments were carried out in 0.1 M CF_3SO_3H (pH = 1.0). $E_{1/2}$ values reported in this work were estimated from CV experiments as the average of the oxidative and reductive peak potentials ($E_{p,a}$ + $E_{p,c}$)/2 or taken as $E(I_{max})$ from DPV or SQWV measurements. For construction of the Pourbaix diagrams, the following buffers were used: dihydrogen phosphate/phosphoric acid up to pH = 4 (pK_a = 2.12), hydrogen phosphate/dihydrogen phosphate up to pH = 9 (pK_a = 7.67), hydrogen phosphate/sodium phosphate up to pH= 13 (pK_a = 12.12) and sodium hydroxide for pH = 14. Also 0.1 M triflic acid was used for pH = 1.0. The concentration of the species was approximately 1 mM. Manometric measurements were performed with home-made water-jacked glass reactor coupled to a Testo 521 manometer. Composition of the gaseous phase was determined by online mass-spectrometry with an OmniStar^{TM} GSD 301 C (Pfeiffer) quadrupole mass-spectrometer. A response ratio of 1:2 was observed when equal concentrations of dioxygen (O_2) and carbon dioxide (CO_2), respectively, were injected and thus was used for calculation of their relative concentrations. Oxygen generation in solution was measured via a water-jacket Clark-electrode reactor from Hansatech. In a typical experiment, 2 mL of a 1 mM complex solution in CF_3SO_3H (pH = 1.0) was degassed with nitrogen until no oxygen could be detected. The reactor was then closed by a septum sealed adapter, which was brought in direct contact to the reaction solution to avoid the existence of a gas phase. A minimum volume of prior degassed Ce(IV) solution, equal to 100 redox equivalents, is added directly into the reaction solution with a Hamilton syringe. Blank experiments were performed by addition of Ce(IV) solution to neat CF_3SO_3H (pH = 1.0) in the absence of catalyst. Chemical redox spectrophotometric titrations were performed by sequential addition of a small volume of a Ce(IV) solution in CF_3SO_3H (pH = 1.0) (50 μL/redox equivalent) to the complex solution (2.5 mL) in standard 1 cm Quartz cuvettes.

Kinetics: Experiments were performed on a Cary 50 spectrophotometer equipped with a temperature-controlled cell holder. In a typical experiment, to a 3 mL solution of **4**$^{4+}$ (0.1 mM) in 0.1 M CF_3SO_3H, 1 equiv of Ce(IV) in 10 μL CF_3SO_3H (pH = 1.0) were added at 25.0 ºC ± 0.1ºC. First order rate constants were calculated by a global fitting method using Specfit.

Light-driven catalytic oxidations: In a typical experiment, a water-jacketed cell containing a deoxygenated aqueous (H$_2$O, 5 mL) solution at pH = 7.04 (0.05 M phosphate buffer) with Ru catalyst (**4**$^{4+}$/**7**$^{4+}$, 0.02 mM), substrate (10 mM) and [Co(NH$_3$)$_5$(Cl)]Cl$_2$ (acceptor, 20 mM) was exposed to a simulated sunlight (λ> 400 nm, UV cut-off filter) for 24 h at 25ºC, a period during which the mixture was kept under magnetic stirring. Throughout these photocatalytic experiments, visible-light irradiation

was provided by a 150W Xe arc lamp. The incident irradiance at the surface of the reaction vessel was approximately 0.3 Wcm^{-2}. The reaction product was characterized by ^{1}H-NMR spectroscopy through quantitative analyses of integrated peak intensities relative to the corresponding reference/substrate. For water oxidation experiments, oxygen generation in solution was measured via a water-jacket Clark-electrode reactor from Hansatech (2 mL solution).

X-ray Crystal Structure Determination. Crystals complexes **4**$(PF_6)_{2.25}(CF_3SO_3)_{0.75}$ and **5**$(PF_6)(Cl)_2{\cdot}(CH_3COCH_3)_3{\cdot}(H_2O)_3$ were obtained by slow evaporation of an acetone/0.1 M triflic acid solution (pH = 1.0) (1/4) mixture and a DCM/MeOH (1/1) solvent mixture, respectively. The measured crystals were prepared under inert conditions immersed in perfluoropolyether as protecting oil for manipulation.

Data collection: Crystal structure determinations were carried out using a Bruker-Nonius diffractometer equipped with an APPEX 2 4K CCD area detector, a FR591 rotating anode with MoK_α radiation, Montel mirrors as monochromator and a Oxford Cryosystem plus low temperature device (T = -173 °C). Full-sphere data collection was used with ω and φ scans. *Programs used:* Data collection APEX-2[16], data reduction Bruker Saint[17] V/.60A and absorption correction SADABS.[18]

Structure Solution and Refinement: Crystal structure solution was achieved using direct methods as implemented in SHELXTL[19] and visualized using the program XP. Missing atoms were subsequently located from difference Fourier synthesis and added to the atom list. Least-squares refinement on F^2 using all measured intensities was carried out using the program SHELXTL. All non hydrogen atoms were refined including anisotropic displacement parameters. Compound **4**$(PF_6)_2(CF_3SO_3)$ crystallizes similarly to a MOF (Metal-Organic-Framework) in a two-dimensional porous structure. The metal organic compound crystallizes in a larger crystalline cell (trigonal space group R-3) which contains two dimensional solvent channels which have a diameter of approximately 21 Å. These channels are filled with highly disordered water molecules. In this channel, for each metal organic molecule, 32 positions of water molecules (without hydrogen atoms) with different occupancies could be refined leading to a model with a R1 value of 8.36 %.In order to avoid the highly disordered solvent molecules the program SQUEEZE was applied leading to a refined model with a R1 value of 6.32 % in which water molecules were removed.[20] In the structure three PF_6 anions could be detected which are disordered interchanging its positions with triflate anions (occupancy ratios PF_6/triflate: 50/50, 85/15 and 90/10). The total occupancy for the PF_6 anions is of 75 %.

Acknowledgements

Support from MINECO (CTQ2010-21497), Generalitat de Catalunya and "la Caixa" Foundation are gratefully acknowledged. SM thanks MINECO for a Torres Quevedo grant.

[1] a) A. Llobet, F. Meyer, *Angew. Chem. Int. Ed*. **2011**, *50*, A30-A33; b) A. Melis *Energy Environ. Sci*. **2012**, *5*, 5531-5539.

[2] a) W. Chen, F. N. Rein, R. C. Rocha, *Angew. Chem. Int. Ed.* **2009**, *121* 9852-9855; b) W. Chen, F. N. Rein, B. L. Scott, R. C. Rocha, *Chem. Eur. J.* **2011**, *17*, 5595-5604; c) O. Hamelin, P. Guillo, F. Loiseau, M. F. Boissonnet, S. Ménage, *Inorg. Chem.* **2011**, *50*, 7952–7954; d) W. Song, C.R.K. Glasson, H. Luo, K. Hanson, M. K. Brennaman, J. J. Concepcion, T, J. Meyer, *J. Phys. Chem. Lett.* **2011**, *2*, 1808-1813; e) P. Guillo, O. Hamelin, G. Batat, G. Jonusauskas, N. D. McClenaghan, S. Ménage, *Inorg. Chem.* **2012**, *51*, 2222-2230; f) D. L. Ashford, D. J. Stewart, C. R. Glasson, R. A. Binstead, D. P. Harrison, M. R. Norris, J. J. Concepcion, Z. Fang, J. L. Templeton, T. J. Meyer, *Inorg. Chem.* **2012**, *51*, 6248-6430.

[3] a) F. Li, Y. Jiang, B. Zhang, F. Huang, Y. Gao, L. Sun, *Angew. Chem. Int. Ed.* **2012**, *51*, 2417–2420; b) N. Kaveevivitchai, R. Chitta, R. Zong, M. El Ojaimi, R. P. Thummel, *J. Am. Chem. Soc.* **2012**, *134*, 10721–10724.

[4] E. Jakubikova, R. L. Martin, E. R. Batista, *Inorg. Chem.* **2010**, *49*, 2975-2982.

[5] a) Y. M. Lee, S. N. Dhuri, S. C. Sawant, J. Cho, M. Kubo, T. Ogura, S. Fukuzumi, W. Nam, *Angew. Chem. Int. Ed*. **2009**, *48*, 1803-1806; b) Y. Hirai, Y. Hirai, T. Kojima, Y. Mizutani, Y. Shiota, K. Yoshizawa, S. Fukuzumi, *Angew. Chem. Int. Ed.* **2008**, *47*, 5772-5776.

[6] a) D. Kalita, B. Radaram, B. Brooks, P. P. Kannam, X. Zhao, *ChemCatChem* **2011**, *3*, 571-573; b) M. Hajimohammadi, N. Safari, H. Mofakham, F. Deyhimi, *Green Chem.* **2011**, *13*,991-997; c) F. Li, M. Yu, Y. Jiang, F. Huang, Y. Li, B. Zhang, L. Sun, *Chem. Commun.* **2011**, *47*, 8949-8951; d) S. Fukuzumi, T. Kishi, H. Kotani, Y. M. Lee, W. Nam, *Nat. Chem.* **2010**, *3*, 38-41.

[7] a) C. R. Arana, H. D. Abruña, *Inorg. Chem.* **1993**, *32*, 194; b) C. M. Hartshorn, N. Daire, V. Tondreau, B. Loeb, T. J. Meyer, P. S. White, *Inorg. Chem.* **1999**, *38*, 3200; c) N. Chanda, B. Sarkar, S. Kar, J. Fiedler, W. Kaim, G. K. Lahiri, *Inorg. Chem.* **2004**, *43*, 5128; d) S. Ghumaan, B. Sarkar, N. Chanda, M. Sieger, J. Fiedler, W. Kaim, G. K. Lahiri, *Inorg. Chem.* **2006**, *45*, 7955; e) R. C. Rocha, F. N. Rein, H. Jude, A. P. Shreve, J. J. Concepcion, T. J. Meyer, *Angew. Chem., Int. Ed.* **2008**, *47*, 503; f) L. M. Vogler, K. J. Brewer, *Inorg. Chem.* **1996**, *35*, 818.

[8] a) X. Sala, E. Plantalech, A. Poater, M. Rodriguez, I. Romero, M. Sola, A. Llobet, S. Jansat, M. Gómez, H. Stoeckli-Evans, J. Benet-Buchholz, *Chem. Eur. J.* **2006**, *12*, 2798–2807; b) X. Sala, I. Romero, M. Rodriguez, A. Llobet, G. Gonzalez, M. Martinez, J. Benet-Buchholz, *Inorg. Chem.* **2004**, *45*, 5403-5409; c) S. Roeser, P. Farràs, F. Bozoglian, M. Martínez-Belmonte, J. Benet-Buchholz, A. Llobet, *ChemSusChem* **2011**, *4*, 197-207

[9] a) K. Takeuchi, M. Thompson, D. Pipes, T. J. Meyer, *Inorg. Chem.* **1984**, *23*, 1845-1851; b) A. Llobet, *Inorg. Chim. Acta* **1994**, *221*, 125-131.

[10] a) C. Sens, I. Romero, M. Rodríguez, A. Llobet, T. Parella, J. Benet-Buchholz, *J. Am. Chem. Soc.* **2004**, *126*, 7798; b) X. Sala, M. Rodriguez, I. Romero, L. Escriche, A. Llobet, *Angew. Chem. Int. Ed.* **2009**, *48*, 2842; c) S. Romain, L. Vigara, A. Llobet, *Acc. Chem. Res.* **2009**, *42*, 1944; d) L. Francas, X. Sala, E. Escudero-Adan, J. Benet-Buchholz, L. Escriche, A. Llobet, *Inorg. Chem.* **2011**, *50*, 2271-2781; e) S. Maji, L. Vigara, F. Cottone, F. Bozoglian, J. Benet-Buchholz, A. Llobet, *Angew. Chem. Int. Ed.* **2012**, *51*, 5967–5970.

[11] D. Wasylenko, C. Ganesamoorthy, M. Henderson, B. Koivisto, H. Osthoff, C. Berlinguette, *J. Am. Chem. Soc.* **2010**, *132*, 16094–16106.

[12] a) C. Sens, M. Rodriguez, I. Romero, A. Llobet, T. Parella, J. Benet-Buchholz, *Inorg. Chem.* **2003**, *42*, 8385-8394; b) E. L. Lebeau, T. J. Meyer, *Inorg. Chem.* **1999**, *38*, 2174-2181; c) V. J. Catalano, R. A. Heck, C. E. Immoos, A. Ohman, M. Hill, *Inorg. Chem.* **1998**, *37*, 2150-2157; d) A. Gerli, J. Reedijk, M. T. Lakin, A. L. Spek, *Inorg. Chem.* **1995**, *34*, 1836-1843.

[13] B. P. Sullivan, J. M. Calvert, T. J. Meyer, *Inorg. Chem.* **1980**, *19*, 1404-1407.

[14] L. M. Vogler, B. Scott, K. J. Brewer, *Inorg. Chem.* **1993**, *36*, 898-903.

[15] L. M. Vogler, K. J. Brewer, *Inorg. Chem.* **1996**, *35*, 818-824.

[16] Data collection with APEX II versions v1.0-22, v2009.1-0 and v2009.1-02. Bruker, **2007**. Bruker AXS Inc., Madison, Wisconsin, USA.

[17] Data reduction with Bruker SAINT versions V.2.10, **2003**, V/.60A and V7.60A. Bruker, **2007**. Bruker AXS Inc., Madison, Wisconsin, USA.

[18] SADABS: V.2.10, **2003**; V2008 and V2008/1 Bruker, **2001**. Bruker AXS Inc., Madison, Wisconsin, USA. *Acta Cryst.* **1995**, *A51*, 33-38.

[19] SHELXTL versions V6.12 and 6.14. G. M. Sheldrick, *Acta Cryst.* **2008**, *A64*, 112-122.

[20] SQUEEZE implemented in Platon. A. L. Spek, *J. Appl. Cryst.* **2003**, *36*, 7-13.

Catch Phrase: Photocatalytic oxidations with Ru

*Pau Farràs, Somnath Maji, Jordi Benet-Buchholz, Antoni Llobet**..... Page – Page

Synthesis, Characterization and Reactivity of Dyad Ru-Based Molecules for Light-Driven Oxidation Catalysis

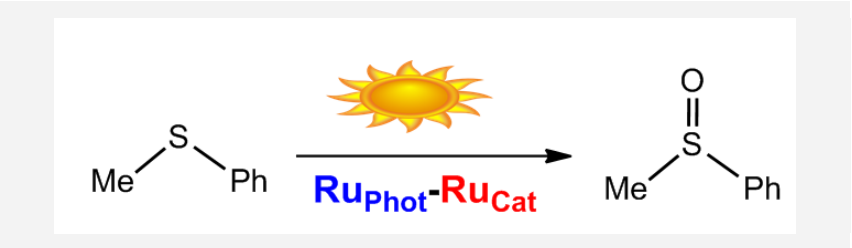

Chemical, electrochemical and phtotochemically induced oxidations of organic substrates is achieved using Ru dinuclear dyad type of complexes, containing a photoactive site and a catalytic site bonded through a bridging ligand.